

5

Ever

Technical Report No. 32-98

Three-Dimensional Optimum Thrust Trajectories

William G. Melbourne

FACILITY FORM 502

N65-82304
(ACCESSION NUMBER)

19
(PAGES)

CR 60972
(NASA CR OR TMX OR AD NUMBER)

(THRU)

the
(CODE)

(CATEGORY)

jpl

JET PROPULSION LABORATORY
CALIFORNIA INSTITUTE OF TECHNOLOGY
PASADENA, CALIFORNIA

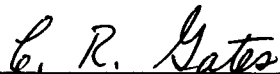
March 15, 1961

410-1

NATIONAL AERONAUTICS AND SPACE ADMINISTRATION
CONTRACT NO. NASW-6

Technical Report No. 32-98
THREE-DIMENSIONAL OPTIMUM
THRUST TRAJECTORIES

William G. Melbourne



C. R. Gates, Chief
Systems Analysis Section

JET PROPULSION LABORATORY
CALIFORNIA INSTITUTE OF TECHNOLOGY
PASADENA, CALIFORNIA
March 15, 1961

Copyright © 1961
Jet Propulsion Laboratory
California Institute of Technology

CONTENTS

I. Optimum Thrust Equations	1
II. Terminal Conditions	6
III. Numerical Results	8
References	10
Figures	11

FIGURES

1. Venus three-dimensional rendezvous trajectory, 120-day heliocentric flight time, ecliptic projection	11
2. Venus three-dimensional rendezvous trajectory, 120-day heliocentric flight time, celestial latitude of the vehicle	11
3. Venus three-dimensional rendezvous trajectory, 120-day heliocentric flight time, thrust program	12
4. Venus three-dimensional rendezvous trajectories, 120-day flight time, variation of $\int_0^{t_1} a^2 dt$ with rendezvous point	12
5. Venus two-dimensional rendezvous trajectories, variation of $\int_0^{t_1} a^2 dt$ with flight time	13
6. Venus three-dimensional rendezvous trajectories, the effect of orbital inclination on $\int_0^{t_1} a^2 dt$	13
7. Venus three-dimensional rendezvous trajectories, variation of minimum and maximum $\int_0^{t_1} a^2 dt$, rendezvous points with flight time	14

FIGURES (Cont'd)

8. Mars three-dimensional rendezvous trajectories, 90-day flight
time, variation of $\int_0^T a^2 dt$ and $M + N$ with rendezvous point 15

THREE-DIMENSIONAL OPTIMUM THRUST TRAJECTORIES

William G. Melbourne¹

ABSTRACT

The three-dimensional equations for optimum variable thrust with power-limited propulsion systems are presented. An iterative routine to solve the two-point boundary value problem has been coupled with these equations to obtain numerical solutions for specified end conditions. A set of interplanetary rendezvous trajectories to Venus is presented, and the effect of orbital inclination for this case is assessed.

I. OPTIMUM THRUST EQUATIONS

The optimum thrust equations of power-limited flight as developed by Irving and Blum⁽¹⁾ have been extended to three dimensions⁽²⁾. These equations arise from the following considerations.

The rocket equation for power-limited propulsion is

$$\frac{1}{m_1} = \frac{1}{m_0} + \int_0^{t_1} \frac{a^2}{2P} dt \quad (1)$$

where m_0 and m_1 are the vehicle masses at the beginning and end, respectively, of the flight, a is the thrust acceleration, and P is the power

¹Research Group Supervisor, Jet Propulsion Laboratory, California Institute of Technology, Pasadena, California.

expended in the rocket exhaust. The exhaust power is determined by the power rating of the powerplant carried by the vehicle and by the efficiency of conversion by the propulsion system. It is evident that m_1 is maximized by minimizing the above integral. The value of this integral depends upon flight time, the mission involved (namely, the specification of the kinematic conditions of the vehicle initially and terminally), the force field in which the vehicle travels, the nature of the thrust program used to accomplish this mission, and, finally, the engineering design of the propulsion system.

For the preliminary mission feasibility studies it is desirable to employ optimum thrust programs which exclude the complexity imposed by the engineering design but which bracket or isolate that class of trajectories and vehicle performances which an actual vehicle would be capable of achieving.

One such thrust program which partially fulfills this need is obtained by satisfying the criterion that the quantity $\int_0^{t_1} a^2 dt$ is a minimum using an unconstrained thrust magnitude. The justification of this program is based on the fact that over a wide range of specific impulse, but excluding lower values, the power conversion efficiency of the propulsion system is nearly constant, thus allowing the removal of P from the integral. Since the thrust magnitude is unconstrained, this program yields the absolute minimum that $\int_0^{t_1} a^2 dt$ may have, and therefore leads to a somewhat optimistic estimate of vehicle payload.

The present studies employ an inverse square central force field model in three dimensions. The equations of motion of a vehicle in such a field may be written in vectorial form as

$$\ddot{\vec{r}} + \nabla V - \vec{a} = \vec{0} \quad (2)$$

where \vec{r} is the position vector, and V is the potential in this force field. The minimization of $\int_0^{t_1} a^2 dt$ may be accomplished by calculus of variations methods in which this integral is minimized subject to certain constraints, namely, the equations of motion, the thrust program constraints, and the initial and terminal kinematic conditions specified by the mission.

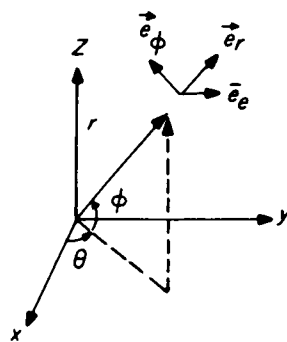
For the variable thrust program it may be shown (2) that the thrust acceleration equations which must be satisfied as necessary conditions for minimum $\int_0^{t_1} a^2 dt$ are

$$\ddot{\vec{a}} + (\vec{a} \cdot \nabla) \nabla V = \vec{0} \quad (3)$$

Since V is not an explicit function of time, these equations admit a first integral in scalar form which may be expressed as

$$\dot{\vec{a}} \cdot \dot{\vec{r}} - \frac{1}{2} a^2 + \vec{a} \cdot \nabla V = \text{constant} \quad (4)$$

Because of the spherical symmetry of this problem it is advantageous to express this result in spherical coordinates. This coordinate system and the direction of the basis vectors are illustrated in the accompanying sketch.



The state variables for this formulation are r , θ , ϕ , u , h_θ , and h_ϕ , where u is radial velocity, and h_θ and h_ϕ are the components of angular momentum per unit mass. The control variables are a_r , a_θ , and a_ϕ . After some manipulation it may be shown that Equations (2) and (3) may be expressed as

$$\dot{u} - \frac{h^2}{r^3} + \frac{\mu}{r^2} - a_r = 0 \quad (5)$$

$$u - \dot{r} = 0 \quad (6)$$

$$\dot{h}_\theta - \frac{h_\phi^2 \tan \phi}{r^2} + r a_\phi = 0 \quad (7)$$

$$\dot{h}_\phi + \frac{h_\theta h_\phi \tan \phi}{r^2} - r a_\theta = 0 \quad (8)$$

$$h_\theta + r^2 \dot{\phi} = 0 \quad (9)$$

$$h_\vartheta - r^2 \dot{\theta} \cos \vartheta = 0 \quad (10)$$

$$h^2 = h_\vartheta^2 + h_\theta^2 \quad (11)$$

$$\ddot{a}_r + \frac{3a_r}{r^4} \left[h^2 - \frac{2\mu r}{3} \right] - \frac{1}{r} \left[a_\theta^2 + a_\vartheta^2 \right] - \frac{2h_\vartheta \tan \vartheta}{r^4} (\vec{h} \cdot \vec{a}) - \frac{h_\theta F(t)}{r^3} - \frac{K_1 h_\vartheta}{r^3 \cos \vartheta} = 0 \quad (12)$$

$$F(t) + 2r^2 \frac{d}{dt} \left[\frac{a_\vartheta}{r} \right] - \frac{4h_\theta a_r}{r} + \frac{2h_\vartheta a_\theta \tan \vartheta}{r} = 0 \quad (13)$$

$$\dot{F}(t) - \frac{2h_\vartheta}{r^3 \cos^2 \vartheta} (\vec{h} \cdot \vec{a}) - \frac{K_1 h_\vartheta \sin \vartheta}{r^2 \cos^2 \vartheta} = 0 \quad (14)$$

$$r^2 \frac{d}{dt} \left[\frac{a_\theta}{r} \right] + \frac{h_\vartheta}{r} (2a_r - a_\vartheta \tan \vartheta) - \frac{\tan \vartheta}{r} (\vec{h} \cdot \vec{a}) - \frac{K_1}{2 \cos \vartheta} = 0 \quad (15)$$

where h is the angular momentum per unit mass of the vehicle, and μ is the gravitational constant of the central body. The quantity $F(t)$ is an auxiliary variable, essentially one of the Lagrange multipliers which could not be easily eliminated. The constant K_1 is a constant of integration resulting from the cyclic nature of the variable θ . Equation (4) becomes

$$a^2 - 2\dot{a}_r \dot{r} + \frac{2a_r}{r^3} \left[h^2 - \mu r \right] - \frac{K_1 h_\vartheta}{r^2 \cos \vartheta} - \frac{h_\theta F(t)}{r^2} - \frac{2h_\vartheta \tan \vartheta}{r^3} (\vec{h} \cdot \vec{a}) = K_2 \quad (16)$$

The quantities K_1 and K_2 are the only constants of motion which have been found. Equation (16) is useful in checking the accuracy of the numerical integrations of Equations (5) - (15). It may be easily verified that these equations reduce to those contained in Reference 1 upon reduction to two dimensions.

II. TERMINAL CONDITIONS

In practice, the state variables are nearly always specified at the initial point of the trajectory and, in fact, many of them usually have specified terminal values. The numerical example to be presented consists of a set of interplanetary rendezvous trajectories commencing from the Earth's heliocentric position and terminating at Venus, whose orbit was considered to be circular but possessing an inclination of $i = 3^\circ.3944$ to the ecliptic plane. This final configuration may be obtained by specifying the terminal values of E , the total energy per unit mass, and h , for a circular orbit, and the value of h_z , the z component of angular momentum. No constraint or specification was placed upon the terminal value of θ , which results in a value of zero for K_1 . It may be shown that certain transversality expressions arise for this case which must be satisfied at the terminal point in order fully to minimize $\int_0^{t_1} a^2 dt$. When the terminal values of E and h are specified, as above, the function $M(t)$, given by

$$M(t) = 2\dot{a}_r\dot{r} + \frac{2a_r}{r^3}(\mu r - h^2) \quad (17)$$

must be zero at t_1 . Moreover, if h_z is specified and ϕ is unspecified, the function $N(t)$, given by

$$N(t) = \frac{2h\phi(\vec{a} \cdot \vec{h})}{r^3} \tan\phi + \frac{h_\theta F(t)}{r^2} \quad (18)$$

must also be zero at t_1 . (For an elliptical terminal orbit, the orientation of the ellipse within the orbit plane is given by the argument of perigee, ω . When E , h , h_z , and ω are specified, it may be shown that $M(t) + N(t)$ must be zero at t_1 .)

The set of equations to be solved is a twelfth-order system and therefore requires the specification of twelve constants of integration. Specification of the six state variables initially leaves six additional constants to define the system. For this numerical example, the specification of the terminal values of E , h , h_z , K_1 , $M(t)$, and either ϕ or $N(t)$ satisfies this requirement. When $N(t_1)$ is zero it may be shown that the value of $\int_0^{t_1} a^2 dt$ is either a relative minimum or maximum with respect to $\phi(t_1)$ (see Fig. 4 and 6). This enables one to obtain the upper and lower bounds in the variation of $\int_0^{t_1} a^2 dt$ for rendezvous at different points on the orbit.

D. E. Richardson of JPL has programmed these equations for numerical solution on an IBM 7090 digital computer. To overcome the two-point boundary value problem associated with this type of equation, an iterative routine designed to efficiently conduct parametric analyses has been developed. This routine has been remarkably successful in the

large-scale production of interplanetary flyby and rendezvous trajectories to nearly all the planets, with flight times ranging from 30 days to 3 years (2).

III. NUMERICAL RESULTS

Fig. 1 illustrates an ecliptic projection of an interplanetary trajectory which will rendezvous Venus in 120 days. The arrows represent the ecliptic projection of \vec{a} at various points along the trajectory. Fig. 2 shows the variation of celestial latitude of the vehicle along this trajectory; the thrust program is presented in Fig. 3. The rendezvous of this particular trajectory is at the optimum point on Venus's orbit, which, for this flight time, is $\emptyset = -3^\circ.189$ on the ascending branch. Because of symmetry, the point $\emptyset = +3^\circ.189$ on the descending branch is also optimum. Fig. 4 exhibits the variation in the value of $\int_0^{t_1} a^2 dt$ with rendezvous at different points along the orbit of Venus. The angle ψ is measured from the ascending node and is related to \emptyset through the expression

$$\sin \emptyset = \sin i \sin \psi \quad (19)$$

The iterative routine mentioned above was used to generate a series of two- and three-dimensional Venus trajectories for a wide range of flight times. Fig. 5 shows the variation in $\int_0^{t_1} a^2 dt$ for a two-dimensional model. The effect of the third dimension due to the inclination of Venus's orbit is exhibited by Fig. 6, in which the increment in $\int_0^{t_1} a^2 dt$ over the

two-dimensional value has been plotted. Both the upper and lower bounds of this increment are included. The variation in ψ for both of these cases is shown in Fig. 7.

In ballistic interplanetary trajectories where velocity impulses are made at the terminal points, it is known that the effects of planetary inclinations on the required velocity increment can be quite severe. It will be observed, however, that this is not the case for advanced propulsion trajectories in which thrust is applied over an extended range. The reason for the comparatively slight effects of inclination is partly due to the small planetary inclinations involved and the relative efficiency with which the advanced system is capable of generating these required inclinations at the terminal point.

Orbital eccentricity has a considerably more prominent effect on $\int_0^{t_1} a^2 dt$, particularly for nearby planets such as Mercury and Mars. Figure 8 illustrates an example of this effect for a set of 90-day rendezvous trajectories to Mars. An orbital eccentricity of 0.0933 and an inclination of 1.85° were adopted; the argument of perigee is -73.9° . The magnitude of the variation of $\int_0^T a^2 dt$ with ψ is about 50% of the average value. The contribution of inclination to this variation is less than 1% of the mean value. This was confirmed by a comparison with an analogous set of two-dimensional trajectories. The transversality expression $M(t) + N(t)$ is included in Fig. 8 and its zero crossings coincide with the maximum and the minimum values of $\int_0^T a^2 dt$.

ACKNOWLEDGEMENT

The author wishes to express his sincere appreciation to D. E. Richardson (JPL), who collaborated in the development of the computer program for these calculations, and to C. G. Sauer (JPL), who made valuable contributions to discussions concerning the analysis.

This paper presents the results of one phase of research carried out at the Jet Propulsion Laboratory, California Institute of Technology, under Contract No. NASw-6, sponsored by the National Aeronautics and Space Administration.

REFERENCES

1. Irving, J., Space Technology, John Wiley and Sons, Inc., 1959, Ch. 10.
2. Melbourne, W. G., Interplanetary Trajectories and Payload Capabilities of Advanced Propulsion Vehicles, Technical Report No. 32-68, Jet Propulsion Laboratory, Pasadena, 1961.

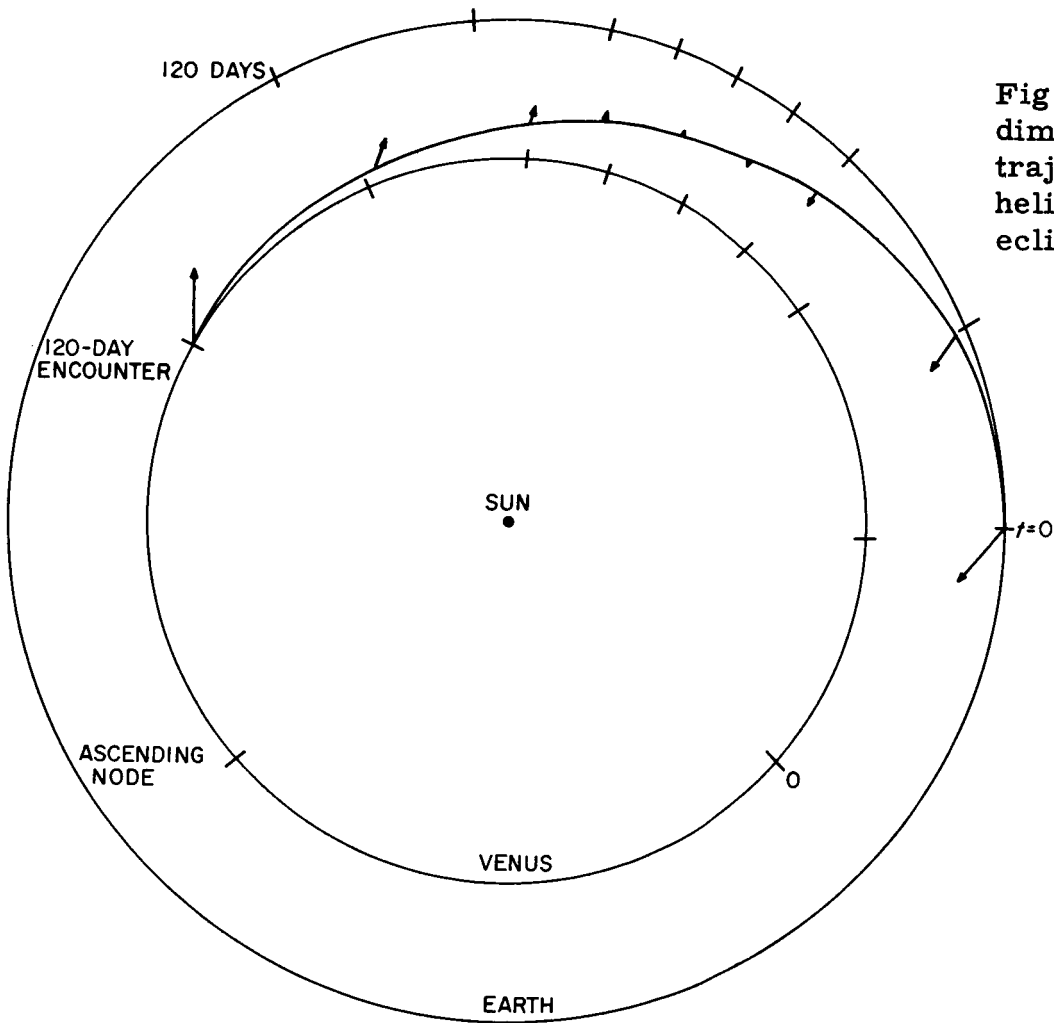
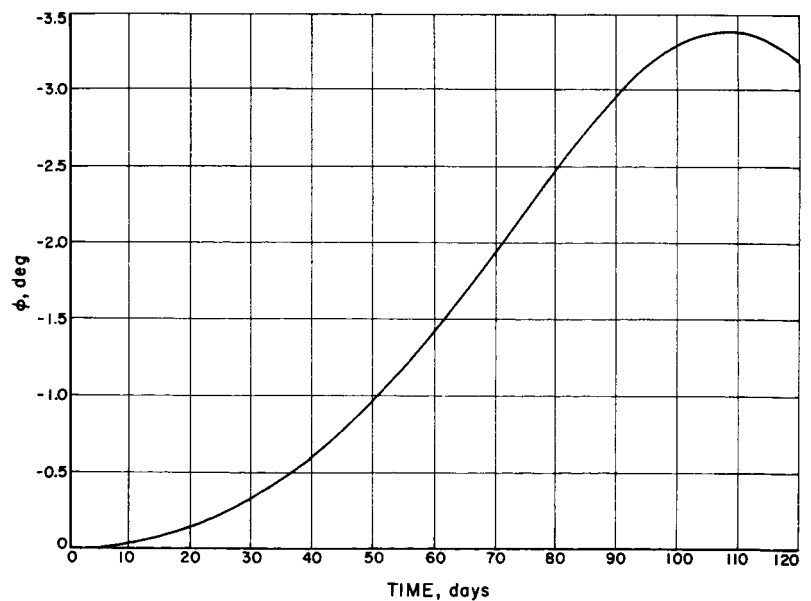


Fig. 1. Venus three-dimensional rendezvous trajectory, 120-day heliocentric flight time, ecliptic projection.

Fig. 2. Venus three-dimensional rendezvous trajectory, 120-day heliocentric flight time, celestial latitude of the vehicle



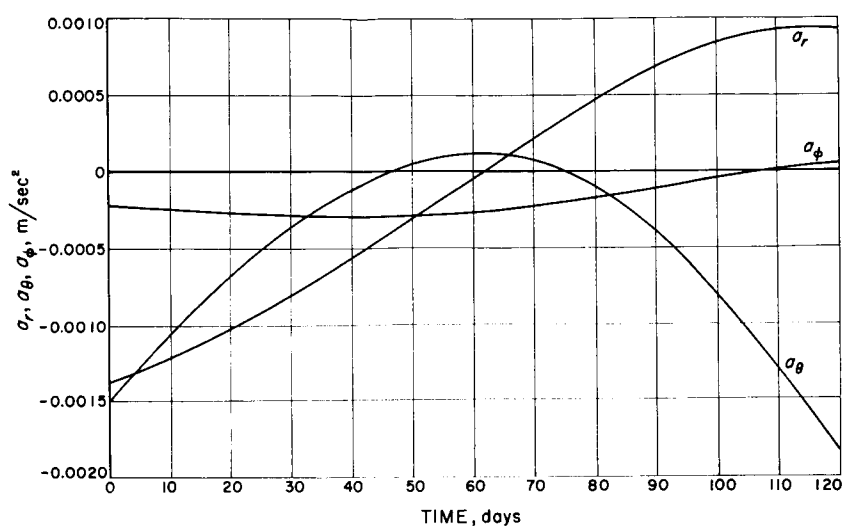


Fig. 3. Venus three-dimensional rendezvous trajectory, 120-day heliocentric flight time, thrust program

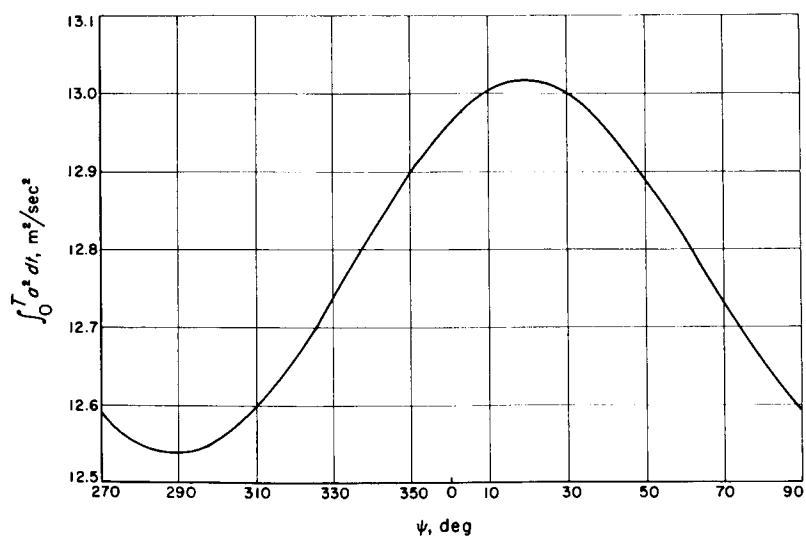


Fig. 4. Venus three-dimensional rendezvous trajectories, 120-day flight time, variation of $\int_0^{t_1} a^2 dt$ with rendezvous point

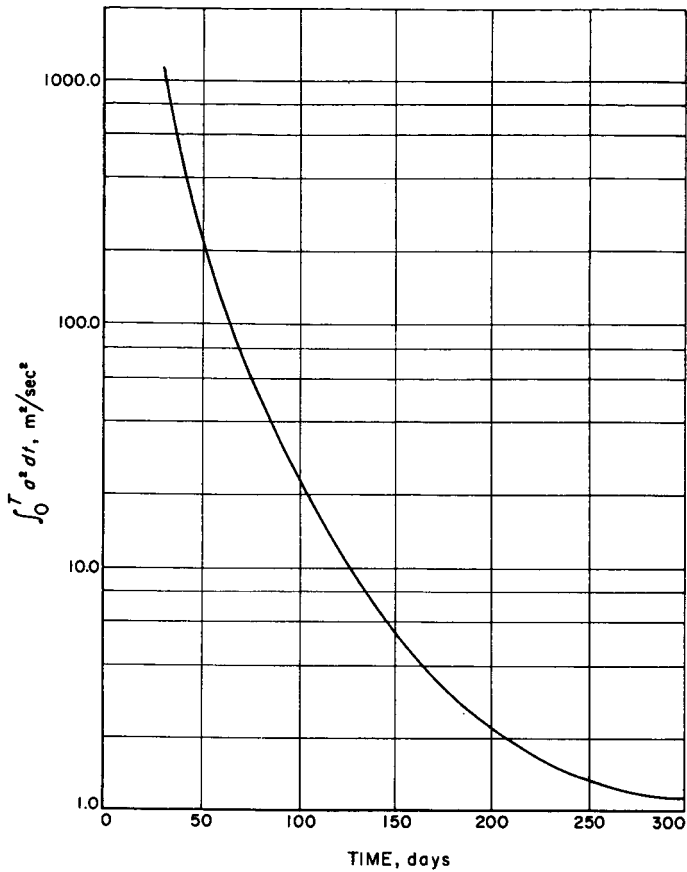
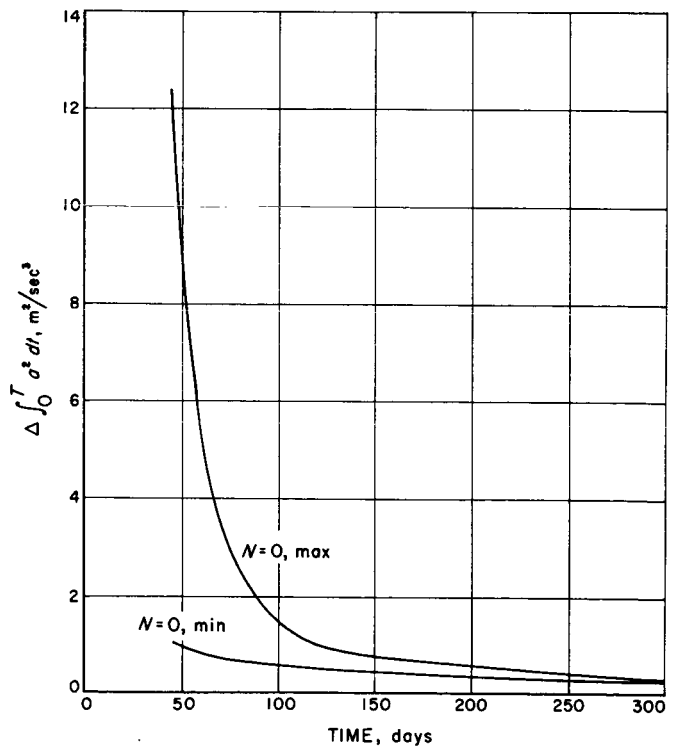


Fig. 5. Venus two-dimensional rendezvous trajectories, variation of $\int_0^{t_1} a^2 dt$ with flight time

Fig. 6. Venus three-dimensional rendezvous trajectories, the effect of orbital inclination on $\int_0^{t_1} a^2 dt$



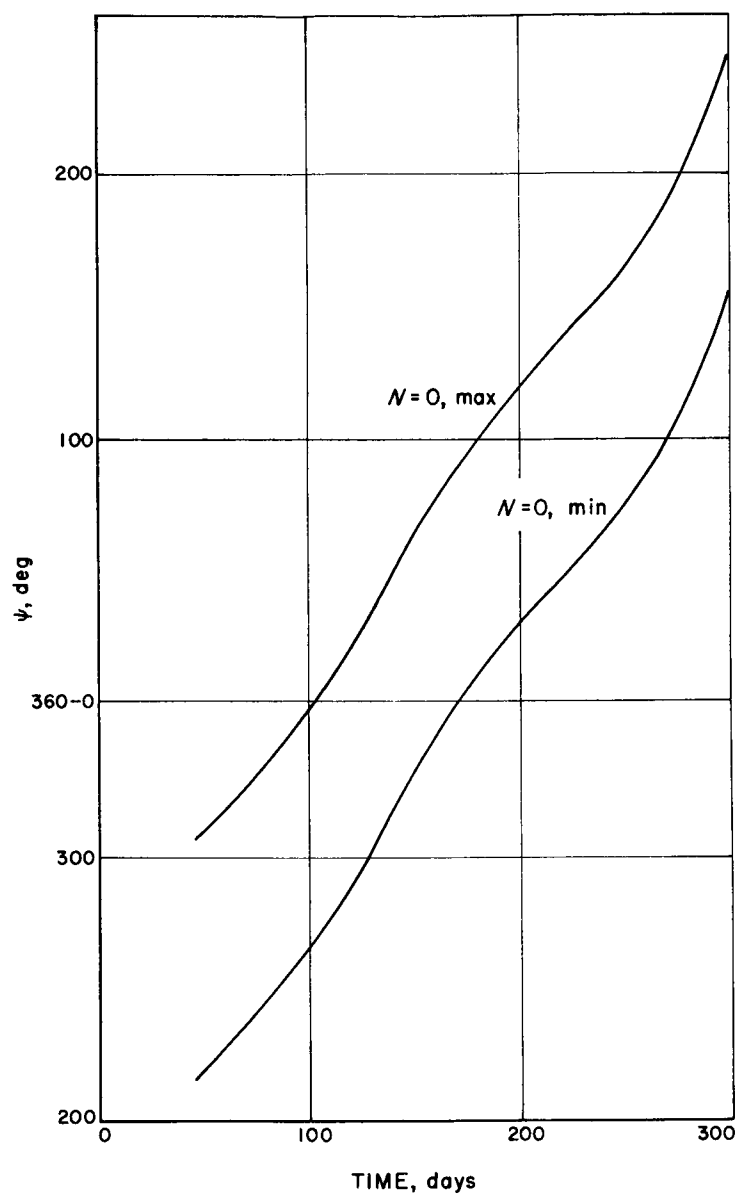


Fig. 7. Venus three-dimensional rendezvous trajectories, variation of minimum and maximum $\int_0^{t_1} a^2 dt$, rendezvous points with flight time

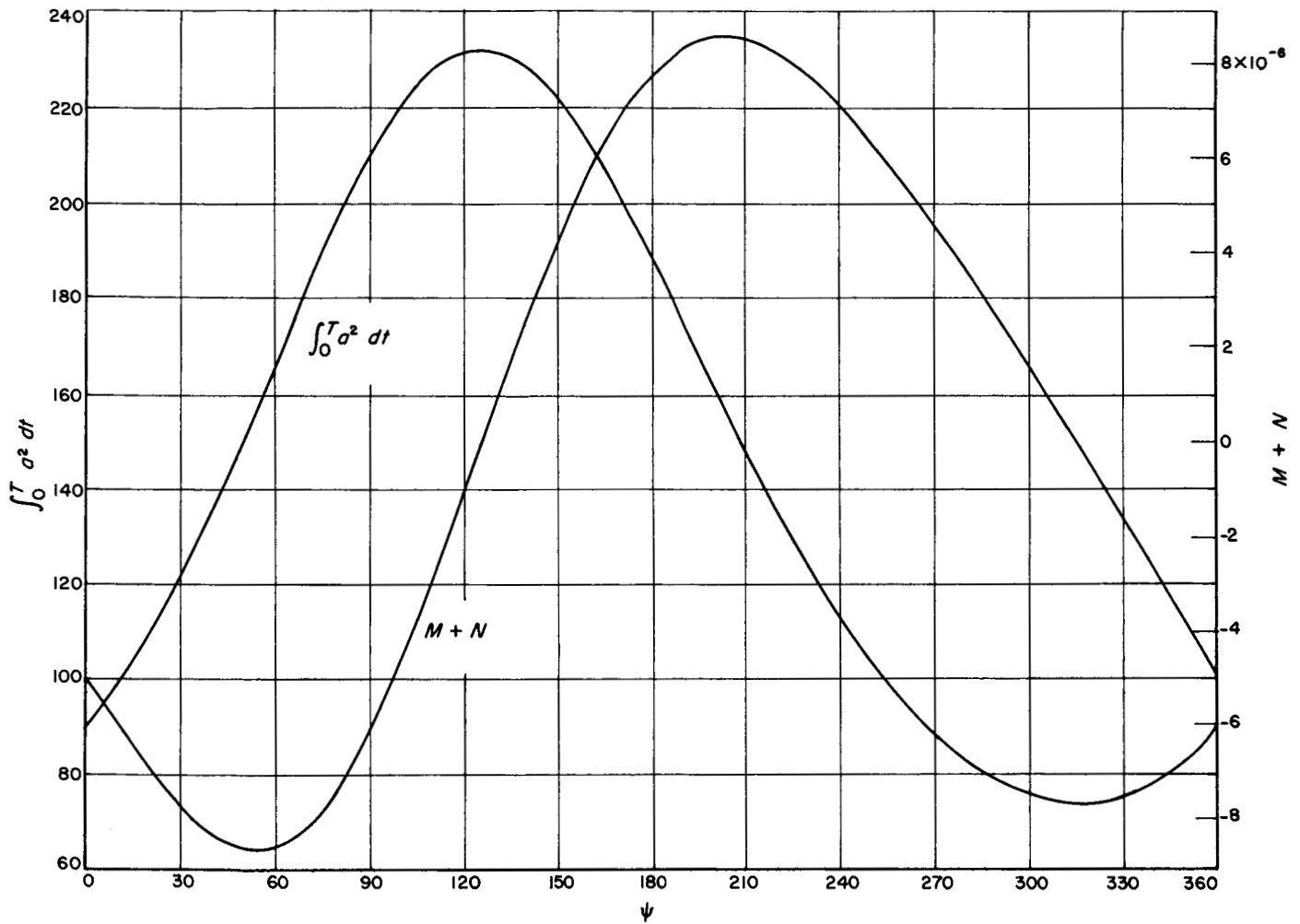


Fig. 8. Mars three-dimensional rendezvous trajectories, 90-day flight time, variation of $\int_0^T a^2 dt$ and $M + N$ with rendezvous point